Traube-Rule Interpretation of Protein Adsorption at the Liquid−Vapor Interface†

Anandi Krishnan,‡ Christopher A. Siedlecki,‡,|| and Erwin A. Vogler*,‡,§

Departments of Bioengineering and Materials Science and Engineering, Pennsylvania State University, University Park, Pennsylvania 16802-5005, and Department of Surgery, Pennsylvania State University College of Medicine, Biomedical Engineering Institute, Hershey, Pennsylvania 17033

Received July 18, 2003. In Final Form: September 22, 2003

Pendant-drop tensiometry of aqueous-buffer solutions of purified human proteins spanning nearly 3 orders of magnitude in molecular weight (MW) reveals that reduction in liquid−vapor (LV) interfacial tension γ_{lv} followed a systematic progression in MW with the molar concentration required to reach a specified γ_{lv} value *decreasing* with *increasing* MW in a manner reminiscent of the Traube rule for linear hydrocarbon surfactants. Furthermore, the concentration dependence of interfacial tension ($d\gamma_{lv}/d \ln C_B$, where C_B is bulk-solution concentration) is observed to be surprisingly invariant among this disparate group of proteins (i.e., approximately constant apparent Gibbs' surface excess $\Gamma = -1/RT\ d\gamma_{lv}/d \ln C_B$). These findings are interpreted through a model of protein adsorption predicated on the interfacial packing of spherical molecules with dimensions scaling as a function of MW. The Traube-rule-like ordering is rationalized as a natural outcome of an invariant partition coefficient that entrains a fixed fraction of bulk-solution molecules within a LV interphase which thickens with increasing protein size (MW). Thus, protein adsorption follows a *homology in molecular size* rather than composition. Calibration of the sphere-packing model to previously reported neutron reflectometry of albumin adsorption permitted interpretation of tensiometric results in terms of interphase thickness and multilayering, predicting that relatively small proteins with MW < 125 kDa (e.g., albumin) fill a single layer whereas larger proteins with MW ∼ 1000 kDa (e.g., IgM) require up to five molecular layers to satisfy a constant partition coefficient.

1. Introduction

Isidor Traube's 1891 investigation of the liquid−vapor (LV) interfacial tension γ_{lv} of hydrocarbon acid, alcohol, ester, and ketone homologues dissolved in water[1] may well be the first systematic observation of what is now commonly known as the hydrophobic effect.[2−4] Traube observed that the molar concentration required to reduce γ_{lv} to an arbitrary value decreased in regular progression with each added methylene unit within a particular homologous series. This pattern eluded Traube's predecessor Emile Duclaux (1840−1904) who, working exclusively in weight/volume (w/v) dilutions, failed to scale concentration-dependent γ_{lv} by solution molarity and discern the pattern that later became evident to Traube.[5] Hence the history of science celebrates the "Traube rule" and remembers Duclaux better by his work with Pasteur and leadership of the Pasteur Institute than his efforts in physical chemistry. Nearly a quarter century later in 1917, Irving Langmuir applied a straightforward thermodynamic interpretation of the Traube rule[6] that systematized existing surfactancy data by assuming that surfactant adsorbed to a planar LV interface as a single molecular layer, with hydrocarbon "tails" protruding through the plane. This insight, which we take quite for granted today, effectively allowed him to estimate the work required to expel a methylene group from aqueous solution (approximately 640 cal/mol).[7] Accordingly, the Traube rule results from the fact that neither "amphilicity" (interaction energetics with water) nor the adsorbed "footprint" of an extended methylene chain (the hydrophobic moiety of a hydrocarbon surfactant) changes significantly within a homologous series and, as a consequence, γ_{lv} scales in a regular and predictable pattern with solution molarity. Thus it is now understood that adsorption of these simple surfactants to the LV interface is effectively dictated by the energetics of hydrophobic hydration.[8]

These water-orchestrated effects were not entirely lost on natural scientists contemporaneous with Langmuir who were just beginning to piece together the now-familiar biochemistry of life (see as examples refs 9, 10, and especially 11 and 12 for a history-of-science perspective). Not fully appreciated then but commonly acknowledged today[5] is that the hydrophobic effect underlies many important biological functions[2,13] such as formation/

* To whom correspondence should be addressed. E-mail: EAV3@PSU.EDU.

† A contribution from the Hematology at Biomaterial Interfaces Research Group, The Pennsylvania State University.

‡ Department of Bioengineering, Pennsylvania State University.

§ Department of Materials Science and Engineering, Pennsylvania State University.

|| Department of Surgery, Pennsylvania State University College of Medicine.

(1) Traube, J. *Annalne Chemie* **1891**, *265*, 27.

(2) Tanford, C. *The Hydrophobic Effect*: *Formation of Micelles and Biological Membranes*; John Wiley & Sons: New York, 1973.

(3) Vogler, E. A. *Adv. Colloid Interface Sci.* **1998**, *74*, 69.

(4) Tanford, C. *Protein Sci.* **1997**, *6*, 1358.

(5) Edsall, J. T. *Proc. Am. Philos. Soc.* **1985**, *129*, 371.

(6) Langmuir, I. *J. Am. Chem. Soc.* **1917**, *39*, 1848.

(7) Adamson, A. W. *Physical Chemistry of Surfaces*, 2nd ed.; Interscience: New York, 1960.

(8) Yaminsky, V. V.; Vogler, E. A. *Curr. Opin. Colloid Interface Sci.* **2001**, *6*, 342.

(9) Macallum, A. B. *Surface Tension and Vital Phenomena*; The University Library: Toronto, 1912.

(10) Henderson, L. J. *The Fitness of the Environment*: *An Inquiry into the Biological Significance of the Properties of Matter*; Macmillan: Boston, 1913.

(11) Vogler, E. A. Biological Properties of Water. In *Water in Biomaterials Surface Science*; Morra, M., Ed.; John Wiley and Sons: New York, 2001; p 4.

(12) Vogler, E. A. On the Origins of Water Wetting Terminology. In *Water in Biomaterials Surface Science*; Morra, M., Ed.; John Wiley and Sons: New York, 2001; p 150.

10.1021/la035308t CCC: $25.00
Published on Web 00/00/0000 PAGE EST: 10.8

Table 1. Purified Proteins

name of protein (acronym)			molecular weight (kDa)	as-received form (mg/mL)	purity (electrophoresis) or activity	vendor
ubiquitin (Ub)			10.7	powder	98%	Sigma Aldrich
thrombin (FIIa)			35.6	powder	1325 NIH unit/mg	Sigma Aldrich
human serum albumin	fraction V (FV HSA)	prep 1	66.3	powder	96−99%	Sigma Aldrich
		prep 2	66.3	powder		Sigma Aldrich
	fatty acid free (FAF HSA)		66.3	powder	96−99%	ICN Biomedicals
prothrombin (FII)	prep 1		72	powder	7.4 units/mg protein	Sigma Aldrich
	prep 2		72	powder		Sigma Aldrich
human IgG (IgG)	prep 1		160	powder	95%	Sigma Aldrich
	prep 2		160	powder	95%	Sigma Aldrich
	prep 3		160	powder	98%	ICN Biomedicals
complement component C1q (C1q)			400	powder	single band by immuno-electrophoresis	Sigma Aldrich
α_2-macroglobulin (α mac)			725	powder	90%	Sigma Aldrich
human IgM (IgM)	prep 1		1000	solution (0.8)	98%	Sigma Aldrich
	prep 2		1000	solution (0.8)	98%	Sigma Aldrich
	prep 3		1000	solution (2.1)	96%	ICN Biomedicals

stability of lipid bilayers, folding of proteins into higher-order structure, and the "biosurfactancy" of proteins[14] that controls adsorption to medical-device surfaces. This latter subject is extremely important in the field of biomaterials, the primary motivation of this work, because it is generally agreed within the biomaterials community that protein adsorption mediates and directs the observed biological response to artificial materials (see refs 15 and 16 and citations therein). Exactly how this occurs at the molecular level is not so clear, however, and protein adsorption remains one of the most controversial and recondite topics in contemporary biomaterials surface science.[14,15,17,18] Failure to come to grips with the protein-adsorption problem is as curious as it is vexing, for one might have otherwise anticipated that water, the universal biological solvent system,[11,18] would impart more obvious regularity in protein adsorption than is readily discernible from the intensive research effort invested in this subject. That is to say, no Traube-like rule for protein adsorption is apparent from decades of focused research, especially as it relates to biocompatibility of materials.

With all of the aforementioned in mind, we have undertaken an extensive study of time- and concentration-dependent γ_{lv} of purified human-protein solutions. A significant motivation of this work was to broaden the scope of previous investigations to include proteins with molecular weight (MW) spanning 3 orders of magnitude in search of a pattern missed in similar previous studies with narrower focus (see especially ref 19 and citations therein). As in these earlier studies, the LV interface was chosen as a molecularly smooth, model hydrophobic surface where interfacial energetics is directly accessible to tensiometric (surface thermodynamic) techniques and adsorbed-protein concentrations Γ can be deduced by application of Gibbs' isotherm.[14] In a manner evocative of the brief history reviewed above, we observe that concentration-dependent γ_{lv} among these diverse proteins is more similar than dissimilar when scaled on a w/v basis whereas molarity scaling reveals a Traube-rule-like ordering[15] by MW at nearly constant Γ.

These results are herein interpreted through a model predicated on the packing of globular-protein molecules having nearly spherical dimensions within the LV surface region. This model explains the Traube-rule-like progression in MW as resulting from adsorption of progressively larger spheres within a commensurately thickening surface region, leading to a homology in *protein size* (rather than methylene units in linear hydrocarbon surfactants). Unlike Langmuir's two-dimensional (2D) interpretation of the interface, which was a good approximation for small-molecule surfactants, the model explicitly treats the surface as a three-dimensional (3D) *interphase* with finite volume that accommodates larger protein molecules. Just as in Langmuir's analysis of hydrocarbon surfactants, however, it is concluded that protein amphilicity does not significantly change within the homologous series in molecular size and, as a consequence, it is possible to rationalize how it happens that γ_{lv} scales with solution molarity at nearly constant Γ. Hence, we find that water does indeed impose discernible regularity in protein adsorption, a factor that may help to better understand the energetics behind the biological response to materials.

2. Methods and Materials

2.1. Purified Proteins. Table 1 compiles pertinent details on proteins and surfactants used as received without further purification. Protein purity was certified by the vendor to be no less than the respective values listed in column 4 of Table 1, as ascertained by electrophoresis (SDS−PAGE or immunoelectrophoresis). Mass, concentration, and molecular weights supplied with purified proteins were accepted without further confirmation. Reference 15 discloses all details related to protein solution preparation including serial dilutions of protein stock solutions (usually 10 mg/mL) that were performed in 96-well microtiter plates by (typically) 50:50 dilution in phosphate-buffered saline (PBS) solution prepared from powder (Sigma Aldrich) in distilled−deionized (18 MΩ) water (the interfacial tension of PBS and water was checked periodically by Wilhelmy balance tensiometry).

2.2. Liquid−Vapor Interfacial Tension Measurements. LV interfacial tensions γ_{lv} reported in this work were measured by pendant-drop tensiometry using a commercial automated tensiometer (First Ten Angstroms Inc., Portsmouth, VA) applying techniques discussed in detail elsewhere.[15] Briefly, the tensiometer employed a Tecan liquid-handling robot to aspirate

(13) Tanford, C. *Science* **1978**, *200*, 1012.
(14) Vogler, E. A. Interfacial Chemistry in Biomaterials Science. In *Wettability*; Berg, J., Ed.; Marcel Dekker: New York, 1993; Vol. 49; p 184.
(15) Krishnan, A.; Sturgeon, J.; Siedlecki, C. A.; Vogler, E. A. *J. Biomed. Mater. Res.* **2003**, in press.
(16) Horbett, T. Protein Adsorption on Biomaterials. In *Biomaterials: Interfacial Phenomena and Applications*; Cooper, S. L., Peppas, N. A., Hoffman, A. S., Ratner, B. D., Eds.; American Chemical Society: Washington, DC, 1982; Vol. 199, p 234.
(17) Vogler, E. A. How Water Wets Biomaterials. In *Water in Biomaterials Surface Science*; Morra, M., Ed.; John Wiley and Sons: New York, 2001; p 269.
(18) Vogler, E. A. *J. Biomater. Sci., Polym. Ed.* **1999**, *10*, 1015.
(19) Tripp, B. C.; Magda, J. J.; Andrade, J. D. *J. Colloid Interface Sci.* **1995**, *173*, 16.

Table 2. Steady-State Protein Parameters

name of protein (acronym)			γ_{lv}^{0} (dyn/cm)	γ'_{lv} (dyn/cm)	ln $C_B^{\Pi/2}$ (pM)	M (dimensionless)	Π^{max} (dyn/cm)	apparent Γ^b (pmol/cm^2)	ln C_B^{max} (pM)
ubiquitin (Ub)[a]			72	46	15		26	146	18
thrombin (FIIa)			72.23 ± 0.31	47.6 ± 1.5	14.44 ± 0.26	−11.00 ± 1.3	24.1 ± 1.5	167 ± 18	17.41 ± 0.18
human serum albumin	fraction V (FV HSA)	prep 1	72.3 ± 1.2	50.3 ± 1.2	12.14 ± 0.28	−9.9 ± 2.5	21.4 ± 1.2	160 ± 21	14.92 ± 0.28
		prep 2	70.8 ± 1.1	46.2 ± 2.5	12.44 ± 0.53	−7.3 ± 2.2	25.5 ± 2.5	129 ± 25	16.26 ± 0.39
	fatty acid free (FAF HSA)		70.83 ± 0.30	53.37 ± 0.47	12.06 ± 0.16	−13.0 ± 2.0	18.33 ± 0.47	167.9 ± 9.4	14.15 ± 0.16
prothrombin (FII)	prep 1		70.50 ± 0.73	43.1 ± 2.4	12.72 ± 0.35	−10.8 ± 2.9	28.6 ± 2.4	207 ± 33	15.39 ± 0.27
	prep 2		70.51 ± 0.73	43.0 ± 2.4	12.72 ± 0.34	−10.8 ± 2.8	28.6 ± 2.4	207 ± 32	15.40 ± 0.26
human IgG (IgG)	prep 1		70.48 ± 0.57	48.7 ± 3.2	13.04 ± 0.69	−8.6 ± 2.1	23.1 ± 3.2	130 ± 34	16.44 ± 0.47
	prep 2		71.13 ± 0.57	51.6 ± 1.9	13.54 ± 0.41	−10.4 ± 2.7	20.1 ± 1.9	134 ± 24	16.49 ± 0.29
	prep 3		71.09 ± 0.42	56.48 ± 0.92	14.65 ± 0.19	−20.1 ± 5.1	15.21 ± 0.92	177 ± 21	16.26 ± 0.17
complement component C1q (C1q)			71.59 ± 0.54	54.2 ± 1.6	11.27 ± 0.38	−14.2 ± 4.1	17.5 ± 1.6	194 ± 33	13.08 ± 0.34
α_2-macroglobulin (α mac)			71.96 ± 0.36	57.21 ± 0.57	9.54 ± 0.15	−19.4 ± 5.7	14.47 ± 0.57	266 ± 21	10.65 ± 0.15
human IgM	prep 1		70.98 ± 0.39	51.4 ± 1.2	9.92 ± 0.19	−13.2 ± 3.5	20.3 ± 1.2	230 ± 26	11.63 ± 0.17
	prep 2		71.65 ± 0.55	50.2 ± 3.1	11.64 ± 0.35	−14.2 ± 4.2	21.5 ± 3.1	232 ± 59	13.50 ± 0.22
	prep 3		70.51 ± 0.59	55.4 ± 1.3	10.58 ± 0.30	−11.7 ± 3.3	16.3 ± 1.3	149 ± 25	12.62 ± 0.26

[a] Ubiquitin (10.7 kDa) does not reach surface saturation within solubility limits; reported values are graphical estimates (see the Appendix, section 6.2). [b] Apparent Γ is proportional to the Gibbs' surface excess Γ_{lv} (see the theory section).

between 10 and 12 μL of solutions contained in a 96-well microtiter plate prepared by the serial-dilution protocol mentioned above. The robot was used to reproducibly transfer the tip with fluid contents into a humidified (99+% relative humidity) analysis chamber and dispense between 6 and 11 μL pendant drops (a smaller drop volume was required for lower interfacial tensions) within the focal plane of a magnifying camera. These and all other aspects of pendant-drop analysis were performed under computer control. The precision of γ_{lv} was about 0.5 dyn/cm based on repeated measurement of the same pendant drop. The instrument was calibrated against pure water interfacial tension and further confirmed on occasion against Wilhelmy balance tensiometry. The analysis chamber was thermostated to a lower limit of 25 ± 1 °C by means of a computer-controlled resistive heater. The upper-temperature limit was, however, not controlled but rather floated with laboratory temperature, which occasionally drifted as high as 29 °C during summer months. Thus, reported γ_{lv} values are probably not more accurate than about 1 dyn/cm on an intersample basis considering the small but measurable variation of water interfacial tension with temperature. This range of accuracy is deemed adequate to the conclusions of this report which do not strongly depend on more highly accurate γ_{lv} that is difficult to achieve on a routine basis. Instead, the veracity of arguments raised herein depends more on a breadth of reliable measurements made across the broad selection of human proteins listed in Table 1. Data analysis and statistical methods are fully described in ref 15.

3. Theory

3.1. General Features of the Protein-Adsorption Model. The protein-adsorption model disclosed below is based on two related experimental observations and implications thereof; namely, (i) the surprisingly slight variation in the concentration dependence of liquid−vapor interfacial tension γ_{lv} among the diverse globular proteins studied herein spanning nearly 3 decades of molecular weight MW (see Tables 1 and 2) and (ii) the substantially constant value of the apparent Gibbs' surface excess Γ for these proteins. The model asserts that these are outcomes of a relatively constant partition coefficient P that entrains protein within an interphase region separating bulk-solution from bulk-vapor phases. The interphase thickens with increasing protein size because the volume occupied by adsorbed-protein molecules is proportional to MW according to the well-known relationships among MW, solvent-exposed area, volume, and packing density.[20] As a consequence, interphase concentrations C_I of larger proteins are lower than that of smaller proteins at constant $P \equiv C_I/C_B$. This latter effect leads directly to a Traube-rule-like ordering for proteins. These principal assertions coupled with a packing model for adsorbed protein provide analytical relationships that, when fitted to experimental data, yield scaling relationships for protein adsorption relating molecular size (MW) to interfacial energetics.

3.2. Liquid−Vapor Interphase. The LV surface region is modeled as a layer with finite thickness bounded by the bulk-vapor phase on one side and by the bulk-solution phase on the other. This "3D" surface-region paradigm is consistent with Gibbs' or Guggenheim constructions and certain venerable adsorption-kinetics models including a subsurface surface region (such as Ward and Tordai)[21] but is not necessarily consistent with a strictly "2D" concept in which all adsorbate is constrained to a single interfacial layer (see refs 3 and 14 and citations therein for more discussion relevant to protein adsorption). More specifically, the interphase is modeled (following Schaaf and Dejardin for example)[22] as consisting of N slabs with thickness δ, the characteristic size of the protein molecule under study (in cm), such that the total interphase thickness (in cm) $\Omega = N\delta$ and volume $V_I = A\Omega = AN\delta$ (in cm^3), where A is the interfacial area (cm^2) and N is an integer number of slabs that may be fully or partially filled. The interphase solute concentration C_I (in mol/cm^3) is related to these variables through eq 1:

$$C_I = n_I/V_I = \left(\frac{n_a + n_B}{AN\delta}\right) = (\Gamma_{lv}/N\delta) + C_B = \Gamma_{lv}/\Omega + C_I/P = \Gamma_{lv}/\Omega\left(\frac{P}{P-1}\right) \approx \Gamma_{lv}/\Omega \quad (1)$$

where n_I is the total number of solute moles (comprised of adsorbate n_a over and above n_B contributed by the bulk phase) that reside within V_I and Γ_{lv} is the Gibbs' surface excess (mol/cm^2). The approximation is specific to the case that adsorption is energetically favorable for which the (dimensionless) partition coefficient $P \equiv C_I/C_B \gg 1$, as generally anticipated for protein adsorption to a hydrophobic interface,[3] so that the bulk-phase contribution to

(20) Richards, F. M. *Annu. Rev. Biophys. Bioeng.* **1977**, *6*, 151.

(21) Ward, A. F. H.; Tordai, L. *J. Chem. Phys.* **1946**, *14*, 453.

(22) Schaff, P.; Dejardin, P. *Colloids Surf.* **1987**, *24*, 239.

n_I is negligible relative to that adsorbed from solution at steady state (i.e., $n_B < n_a$; C_I is dominantly adsorbate). As will be discussed in greater detail below, Γ_{lv} generally differs from the apparent Γ deduced directly from experimental measurements.

3.3. Proteins and Protein Packing within the LV Interphase. Oblate-spheroid, globular-protein molecules are approximately spherical in aqueous solution[4,23] and are consequently modeled as spheres with radius $r_v = 6.72 \times 10^{-8}\mathrm{MW}^{1/3}$ (packing-volume radius in cm for MW expressed in kDa; see ref 20 for a review of the literature up to 1977 and refs 24−29 for subsequent work regarding spherical dimensions and molecular packing of proteins). This strategy is similar to that adopted by Ostuni et al.[30] in which sphere packing is taken to be the simplest physically relevant model intended to yield a semiquantitative description of general trends in protein adsorption. This model is not expected to account for the myriad complexity and variations among proteins that no doubt invalidate spheric assumptions at a detailed level of investigation. Thus, we assume that spherical dimensions apply approximately to proteins with 10 < MW < 1000 kDa, although we have no specific evidence for this other than the above-cited literature and the extent to which the derived model simulates or fits experimental data. With these molecular dimensions, the highest conceivable solution concentration of protein corresponds to face-centered-cubic (FCC, or equivalently hexagonal) close packing of spheres with radius r_v. Such a close-packed unit cell contains eight $^1/_8$ spheres and six $^1/_2$ spheres (total of 4 spheres) residing within a cubic volume $(2r_v\sqrt{2})^3$, and hence the FCC protein concentration $C_{FCC} = 4$ molecules/$(2r_v\sqrt{2})^3$. Using human serum albumin (HSA) as an example protein with MW = 66.3 kDa and calculated r_v = 2.7 nm, C_{FCC} = 14.6 mM (or about 24× physiological concentration;[31,32] ln C_{FCC} = 23.4 in pM). Such high concentrations are not at all likely either in bulk solution or within the interphase. However, it seems reasonable to propose that the maximal interphase concentration C_I^{max} is proportional to C_{FCC} through a packing-efficiency parameter ϵ that effectively measures how close protein spheres can pack, such that $C_I^{max} = \epsilon C_{FCC}$. We assume that packing within an aqueous interphase is limited by repulsion of hydrated spheres[33] and, as a consequence, regard ϵ as a generic factor independent of protein (sphere) size that is approximately constant for all globular proteins discussed herein. If sphere repulsion is uniform and symmetric, then C_I^{max} effectively results from packing spheres with radius $R = \chi r_v$, where χ is a factor measuring the excluded volume surrounding each molecule. Given that $C_{FCC} = 4$ molecules/$(2r_v\sqrt{2})^3$ and $C_I^{max} = 4$ molecules/$(2R\sqrt{2})^3 = \epsilon C_{FCC}$, it follows that $\chi = \epsilon^{-1/3}$. Hence, molecular dimensions $(2r_v)$ differ from the characteristic dimensions $\delta = 2r_v\chi = 2r_v\epsilon^{-1/3}$.

It is of interest to express the protein-packing concepts discussed above in terms of volume fractions as a means of probing further the physical meaning of ϵ. The volume fraction occupied by protein $\Phi_p = n_I V_p/V_I = C_I V_p$, where the protein molar volume $V_p = 4/3\pi r_v^3 N_A$ if N_A is the Avogadro number. At interphase saturation, $C_I = C_I^{max}$ so that $\Phi_p^{max} = 0.74\epsilon$, revealing that Φ_p^{max} is equivalent to FCC packing at $\epsilon = 1$ (by model construction) and decreases linearly with (fractional) ϵ. Φ_p^{max} is independent of MW because the efficiency of packing spheres does not depend on size, even though the volume occupied by large spheres is greater than that of small spheres. Thus, the protein-packing model views adsorption as a process leading to displacement of a fixed amount of water that is controlled by ϵ and that interphase capacity for protein is controlled by the energetics of what amounts to be interphase dehydration.[34]

3.4. A Traube-Like Rule for Protein Adsorption. Equation 2 combines the notion of C_I^{max} with the MW-dependent radius of spherical proteins, where experimentally convenient dimensions of picomolarity (10^{-12} mol/L) have been introduced:

$$C_I^{max} = \frac{\epsilon(4\ \text{molecules})}{(2r_v\sqrt{2})^3} = \frac{0.177\epsilon\ \text{molecules}}{(6.72 \times 10^{-8}\mathrm{MW}^{1/3})^3} = \frac{9.68 \times 10^{11}\epsilon}{\mathrm{MW}}\ (\text{pmol/L}) \quad (2)$$

It is apparent from eq 2 that maximal interphase protein concentration varies inversely with protein size (MW), with higher concentrations for low-MW proteins and sharply lower concentrations for higher-MW proteins. Interphase saturation occurs at C_I^{max} and must therefore correspond to the bulk concentration C_B^{max} at which the limiting interfacial tension γ'_{lv} is achieved (i.e., the concentration at maximum spreading pressure $\Pi^{max} \equiv \gamma_{lv}^0 - \gamma'_{lv}$). C_B^{max} can be estimated from concentration-dependent γ_{lv} curves (see the Appendix, section 6.1) and is related to C_I^{max} through the partition coefficient $P \equiv C_I^{max}/C_B^{max}$. Equation 3 states this relationship as a logarithmic expression that is convenient to apply to (steady-state) concentration-dependent γ_{lv} data:

$$\ln C_B^{max} = \ln(C_I^{max}/P) = \ln(9.68 \times 10^{11}) - \ln \mathrm{MW} + \ln(\epsilon/P) = -\ln \mathrm{MW} + [27.6 + \ln(\epsilon/P)] \quad (3)$$

Assuming that ϵ/P is constant for all proteins within this study (as discussed above for ϵ and below for P), eq 3 predicts a linear relationship between ln C_B^{max} and ln MW with a slope of −1. A value for the unknown ratio ϵ/P can be extracted from the intercept (see Results and Discussion).

Traube's rule for hydrocarbon surfactants stipulates that the concentration required to reduce γ_{lv} to an arbitrary value γ_{lv}^* decreases in a regular progression with each $-CH_2-$ unit (i.e., MW) in a homologous series.[1,2,4,7] Gibbs' adsorption isotherm can be combined with eq 3 to derive a Traube-like rule for proteins by noting that the apparent Gibbs' surface excess Γ is approximated by the slope of

(23) Teller, D. *Nature* **1976**, *260*, 729.
(24) Chothia, C. *Nature* **1975**, *254*, 304.
(25) Miller, S.; Lesk, A.; Janins, J.; Chothia, C. *Nature* **1987**, *328*, 834.
(26) Miller, S.; Janin, J.; Lesk, A.; Chothia, C. *J. Mol. Biol.* **1987**, *196*, 641.
(27) Tsai, J.; Taylor, R.; Chothia, C.; Gerstein, M. *J. Mol. Biol.* **1999**, *290*, 253.
(28) Gerstein, M.; Chothia, C. *Proc. Natl. Acad. Sci. U.S.A.* **1996**, *93*, 10167.
(29) Miller, S.; Janin, J.; Leak, A. M.; Chothia, C. *J. Mol. Biol.* **1987**, *196*, 641.
(30) Ostuni, E.; Grzybowski, B. A.; Mrksich, M.; Roberts, C. S.; Whitesides, G. M. *Langmuir* **2003**, *19*, 1861.
(31) Anderson, N. L.; Anderson, N. G. *Mol. Cell. Proteomics* **2002**, *1*, 845.
(32) Putnam, F. W. Alpha, Beta, Gamma, Omega − The Roster of the Plasma Proteins. In *The Plasma Proteins*: *Structure, Function, and Genetic Control*; Putnam, F. W., Ed.; Academic Press: New York, 1975; Vol. 1, p 58.
(33) Werner, P.; Caflisch, A. *J. Am. Chem. Soc.* **2003**, *125*, 4600.
(34) This conclusion is in general accord with a relatively new theory of protein adsorption introduced by Rao that concludes adsorption is driven by reduction in interfacial water chemical potential. See: Rao, C. S.; Damodaran, S. *Langmuir* **2000**, *16*, 9468.

the linear-like region of experimental concentration-dependent γ_{lv} curves[35,36] (i.e., the "surface excess region" falling between γ^0_{lv} and γ'_{lv} centered at ln $C_B^{\Pi/2}$; see Figure 1A annotations):

$$\delta\gamma_{lv}/\delta \ln C_B = -RT\Gamma \approx \Delta\gamma_{lv}/\Delta \ln C_B = \frac{(\gamma'_{lv} - \gamma^*_{lv})}{[\ln C_B^{max} - \ln C^*_B]} \quad (4)$$

$$\gamma^*_{lv} = \gamma'_{lv} + RT\Gamma[27.6 + \ln(\epsilon/P) - \ln C^*_B - \ln MW] \quad (4a)$$

where C^*_B is the concentration required to achieve any arbitrary γ^*_{lv} within the surface-excess region. Equation 4a follows directly from eq 4 by insertion of eq 3 and is a Traube-like rule for globular proteins where the homology is in *protein size* rather than methylene units in linear surfactants. This size homology results directly from the proportional increase in protein volume with MW.[20]

3.5. Protein Partition Constant. A central assumption of this work is that the partition coefficient P is approximately constant for all proteins. The Guggenheim interphase construction[37,38] can be used to explore this notion more explicitly; for a two-component solution (surface-active solute 2 and solvent 1), the concentration dependence of the liquid−vapor interfacial tension is given by eq 5:

$$\delta\gamma_{lv}/\delta \ln x_2 = \frac{-RT}{A}\left[n^I_2 - \left(\frac{x_2}{x_1}\right)n^I_1\right] \approx \frac{-RT}{A}\left[n^I_2 - \left(\frac{n^I_1}{n_1}\right)n_2\right] \quad (5)$$

where the superscript I differentiates the interphase region from the bulk phase (with no superscript), n is the number of moles of 1 or 2, and x is the mole fraction. The approximation applies to dilute-solute solutions where $x_2 = n_2/(n_1 + n_2) \sim n_2/n_1$ and $x_1 \sim 1$. Equation 5 can be written in terms of solvent and solute partition coefficients $P_1 \equiv C_{I,1}/C_{B,1} = (n^I_1/n_1)(V/V_I)$ and $P_2 \equiv C_{I,2}/C_{B,2} = (n^I_2/n_2)(V/V_I)$, respectively:

$$\delta\gamma_{lv}/\delta \ln x_2 = \frac{-RTC_{B,2}V_I}{A}[P_2 - P_1] = -RTC_{B,2}\Omega[P_2 - P_1] \approx -RTC_{B,2}\Omega[P_2 - 1] \quad (6)$$

where V_I is the interphase volume used as above, V is the bulk-solution volume, and the identity $V_I = A\Omega$ has been applied. The approximation is valid for a dilute-solute solution for which the change in solvent concentration within the interphase due to adsorption is negligible. Equation 6 is valid for any two proteins i and j that might have quite different MWs ($MW_j \neq MW_i$) but which we observe experimentally to exhibit similar $\delta\gamma_{lv}/\delta \ln x_2$ (i.e., the apparent Gibbs' surface excess is approximately constant for all proteins). Simultaneous solution of these two equations using i and j in place of the generic 2 solute designation of eq 6 for the particular situation $C_{B,2} = C_B^{max}$ allows solution for the partition coefficients P_i and P_j in terms of interphase thickness and bulk concentrations:

$$\frac{[P_j - 1]}{[P_i - 1]} = \left(\frac{\Omega^{max}_i}{\Omega^{max}_j}\right)\left(\frac{C^{max}_{B,i}}{C^{max}_{B,j}}\right) = \left(\frac{\Gamma/C^{max}_{I,i}}{\Gamma/C^{max}_{I,j}}\right)\left(\frac{C^{max}_{B,i}}{C^{max}_{B,j}}\right) = P_i/P_j \quad (7)$$

where eq 7 makes use of the approximation $C_I = n_I/V_I \approx \Gamma/\Omega$ that is commensurate with $P \gg 1$. Thus eq 7 leads to the conclusion that $P_j(P_j - 1) = P_i(P_i - 1)$, a condition that can be met only if $P_i = P_j$. Evidently then, a similar $d\gamma_{lv}/d \ln C_B$ means that the partition coefficient $P \equiv C_I/C_B$ is approximately constant among proteins spanning nearly 3 decades in MW and does not significantly vary with molecular size.

3.6. Surface Excess. An issue that arises in the quantitative interpretation of concentration-dependent LV interfacial tensions is that activity coefficients, even of simple hydrocarbon solutes, are not typically unitary as is frequently assumed in the application of Gibbs' adsorption isotherm, and deviations from ideality have a significant impact on computed values of the Gibbs' surface excess.[39] Proteins are complex polyelectrolyte solutes that are not ideal[40,41] and for which assumption of unit activity coefficients is no doubt quantitatively in error and apparently leads to a considerable difference between real ($\Gamma_{lv} = -1/RT\ d\gamma_{lv}/d \ln a$ where a is solute activity) and apparent ($\Gamma = -1/RT\ d\gamma_{lv}/d \ln x_2$, not corrected for solute activity) surface excess values. However, in this particular work, it is experimentally observed that Γ is approximately constant for proteins with widely varying MW, strongly suggesting that any activity-related discrepancy between Γ and Γ_{lv} is roughly constant among these proteins. The ratio Γ/Γ_{lv} measures this discrepancy and can be written in terms of an activity coefficient $\sigma \equiv a/x_2$ by noting that $\Gamma_{lv} = -a/RT\ (d\gamma_{lv}/da)$ and $\Gamma = -x_2/RT\ (d\gamma_{lv}/dx_2)$:

$$\Gamma/\Gamma_{lv} = (x_2\ d\gamma_{lv}/dx_2)(da/a\ d\gamma_{lv}) = x_2/a(da/dx_2) = 1/\sigma(d\sigma/dx_2) \approx c \quad (8)$$

Thus, $\Gamma_{lv} = c\Gamma$ under the circumstance that the (generally unknown) activity coefficient σ is not a strongly nonlinear function of protein concentration.

3.7. Interphase Thickness. The maximal interphase thickness Ω^{max} that occurs when the interphase is saturated with adsorbate can be computed from eq 1 in combination with eq 2, assuming that $c\Gamma = \Gamma_{lv}$:

$$\Omega^{max} = c\Gamma/C^{max}_I = \frac{c\Gamma\ MW}{9.68 \times 10^8\epsilon} \quad (9)$$

where units of picomoles and centimeters have been used. Equation 9 states that Ω^{max} increases in direct proportion to protein MW (i.e., proportional to protein volume), with a relatively thin interphase for low-MW (smaller) proteins and a thicker interphase for high-MW proteins. Ω^{max} may be comprised of multiple layers as dictated by the partition coefficient P and layer packing calculated from $N^{max} = \Omega^{max}/\delta = \Omega^{max}/2r_v\chi$.

4. Results and Discussion

This portion of the paper is divided into two main parts. The first reports experimental observation of time- and concentration-dependent LV interfacial tension γ_{lv} of

(35) Vogler, E. A. *Langmuir* **1992**, *8*, 2005.
(36) Vogler, E. A. *Langmuir* **1992**, *8*, 2013.
(37) Guggenheim, E. A. *Thermodynamics*: *An Advance Treatment for Chemists and Physicists*, 5th ed.; Wiley: New York, 1967.
(38) Aveyard, R.; Haydon, D. A. *An Introduction to the Principles of Surface Chemistry*; Cambridge University Press: London, 1973.
(39) Strey, R.; Vilsanen, Y.; Aratono, M.; Kratohvil, J. P.; Yin, Q.; Friberg, S. E. *J. Phys. Chem. B* **1999**, *103*, 9112.
(40) Wills, P. R.; Comper, W. D.; Winzor, D. J. *Arch. Biochem. Biophys.* **1993**, *300*, 206.
(41) Knezic, D. Thermodynamic Properties of Supersaturated Protein Solutions. Ph.D. Thesis, Polytechnic University, New York, NY, 2002.

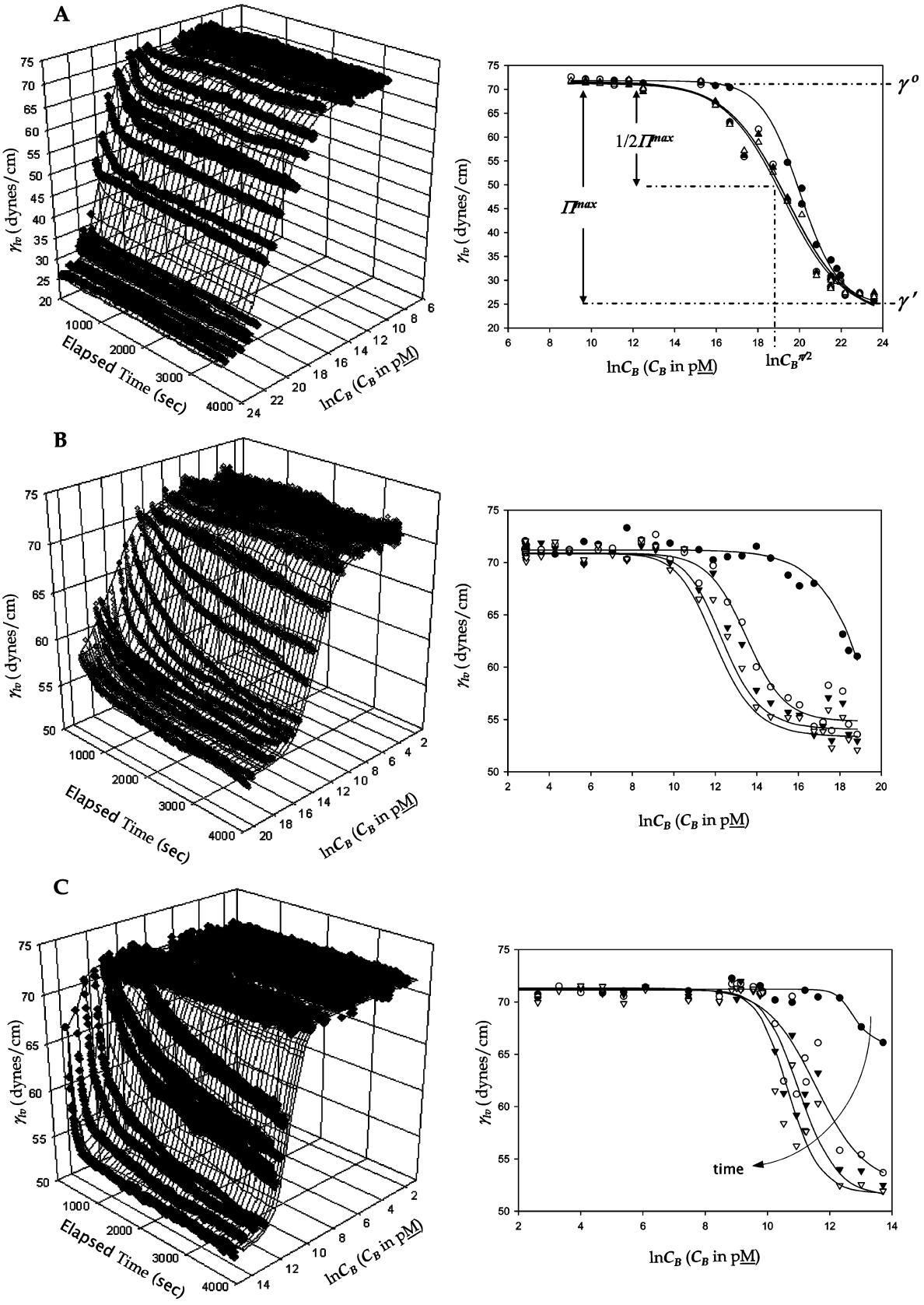

Figure 1. Interfacial tension profiles in 3D (γ_{lv} as a function of analysis time (drop age) and logarithmic (natural) solution concentration C_B) and 2D (γ_{lv} as a function of logarithmic solution concentration C_B at selected times) formats comparing Aerosol-OT (panel A), human serum albumin (panel B), and human immunoglobulin M (panel C, preparation 3, Table 1). In each case, solute concentration C_B is expressed in pmol/L (pM). The symbols in the 2D panels represent time slices through the 3D representations (filled circles = 0.25 s, open circles = 900 s, filled triangles = 1800 s, and open triangles = 3594 s; annotations in panel A indicate maximum and half-maximum spreading pressure). Notice that adsorption kinetics dominates IgM adsorption, requiring 1 h to reach steady state, whereas kinetics dampens within about 2000 s for HSA. Dynamic effects dampen within 900 s for AOT, the small-molecule reference surfactant.

aqueous-buffer solutions of purified human proteins with MW spanning nearly 3 orders of magnitude. The second part interprets these results according to the sphere-packing model in the general order disclosed in the preceding theory section. Taken together, experiment and theory support the contention that water imposes uniformity in protein adsorption to the LV interface, packing molecules into an interphase region that thickens with increasing protein size (MW) at a constant partition coefficient.

4.1. Experimental Results. *Concentration-Dependent LV Interfacial Tension.* The principal experimental observations of this work were time- and concentration-dependent LV interfacial tension γ_{lv} of aqueous-buffer solutions of purified human proteins with MW spanning 3 orders of magnitude. Interfacial tension measurements were made using pendant-drop tensiometry as described in Methods and Materials. Figure 1 compares selected results for the anionic surfactant Aerosol-OT (Figure 1A, AOT, MW = 444 Da), human serum albumin (Figure 1B, fatty-acid-free FAF HSA, MW = 66.3 kDa), and immunoglobulin M (Figure 1C, IgM, 1000 kDa) in both three-dimensional (γ_{lv} as a function of time and concentration) and two-dimensional (γ_{lv} as a function concentration at specified times) representations, termed "γ_{lv} curves" herein. Note that the logarithmic-solute-concentration ordinate ln C_B in Figure 1 is expressed in picomolarity units (pM, 10^{-12} mol solute/L solution). It was observed that these γ_{lv} curves were generally sigmoidal in shape, with well-defined low-concentration limits γ^0_{lv} and high-concentration asymptotes γ'_{lv}. Smooth curves through the data of Figure 1 result from least-squares fitting of a four-parameter logistic equation ($\gamma_{lv} = \{[(\gamma^0_{lv} - \gamma'_{lv})/(1 + (\ln C_B^{\Pi/2}/\ln C_B)^M] + \gamma'_{lv}\}$) to concentration-dependent γ_{lv} data for each time within the observation interval, as described elsewhere.[15,35,36] Empirical application of a logistic equation was a purely pragmatic approach aimed at quantifying variable parameters with a measure of statistical confidence. In this way, data fitting recovered γ^0_{lv}, γ'_{lv}, and a parameter measuring concentration at half-maximal change in interfacial activity, ln $C_B^{\Pi/2}$ (where $\Pi/2 = {}^1/_2\Pi^{max}$ and $\Pi^{max} \equiv \gamma^0_{lv} - \gamma'_{lv}$), as well as a parameter M that measured the steepness of the sigmoidal curve. Results for HSA and IgM (Figure 1B,C, respectively) were similar to those for AOT in that sigmoidal-shaped γ_{lv} curves connected low- and high-concentration asymptotes. Significantly more pronounced time dependence in γ_{lv} was observed for proteins, however, especially for intermediate concentrations.

The dynamics was undoubtedly due to rate-limiting, mass-transfer and adsorption steps that slowly brought large macromolecules to the LV interface relative to the small-molecule reference compound AOT for which only limited kinetics was observed. Observation of time dependence was important in this particular work only insofar as data demonstrate that γ_{lv} kinetics dampened within the time frame of experimentation and achieved steady state within the 3600 s observation window. Data collected in Table 2 refer only to steady-state measurements. The bulk-solution concentration at which the limiting interfacial tension γ'_{lv} occurs (C_B^{max}) is of theoretical interest in this work and was estimated from fitted parameters compiled in Table 2 as described in the Appendix, section 6.1. C_B^{max} is typically interpreted as the critical micelle concentration (cmc), at least for surfactants. This paper provides no evidence of micelles, for either proteins or surfactants, and so only acknowledges a bulk-phase concentration at which further increase in solute concentration did not significantly change γ_{lv}.

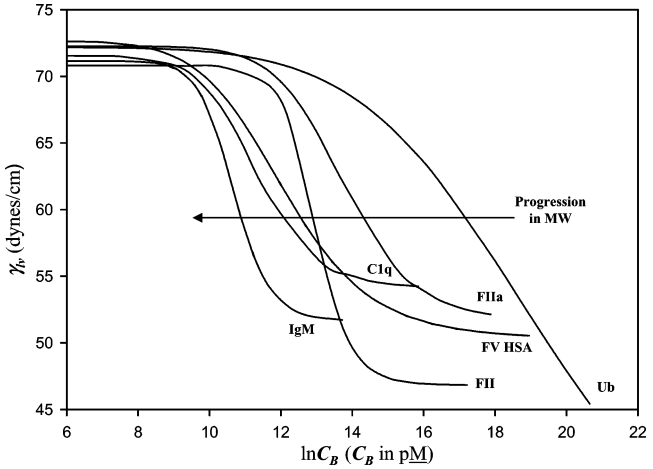

Figure 2. Comparison of steady-state, concentration-dependent γ_{lv} for proteins selected from Table 1 spanning 3 decades in MW (only statistically fit curves are shown for clarity; see Figure 1 for similar plots including authentic data and Table 2 for statistics of fit). Molar scaling reveals a Traube-rule-like ordering in which it is observed that high-MW proteins reduce γ_{lv} to any arbitrary value at lower molarity than low-MW proteins (arrow).

Figure 2 compiles smoothed, steady-state γ_{lv} curves for proteins selected from Table 2 spanning 3 decades in MW (data are not shown in Figure 2 for the sake of clarity; see Figure 1 for examples with authentic data and Table 2 for statistics of fit). The Traube-rule-like progression in MW evident in the molar scaling of Figure 2 was not at all obvious on a w/v basis (not shown) because data are compressed into a single band.[15] However scaled, the similarity of γ_{lv} curves for such a diverse group of proteins is rather striking ($\Pi^{max} < 30$ dyn/cm with γ'_{lv} lying within ± 10 dyn/cm) and corroborates results of previous studies of proteins covering a narrower range of MW.[19] Bearing in mind that the Π^{max} range for synthetic surfactants can exceed 60 dyn/cm, with $25 < \Pi^{max} < 50$ dyn/cm typical of ordinary hydrocarbon soaps and surfactants,[42,43] it is apparent from the data of Table 2 and Figures 1 and 2 that aqueous-protein solutions are relatively weak surfactant systems with Π^{max} only slightly overlapping with the weakest of surfactant systems. In view of the substantial structural diversity of the human plasma proteome sampled by the proteins of Table 1,[31] it seems reasonable to conclude that variability in protein structure does not confer widely varying LV interfacial activity, at least not in comparison to the full range available to ordinary surfactants.

Apparent Gibbs' Surface Excess. The apparent values for the Gibbs' surface excess Γ with error estimates collected in Table 2 were calculated from the slope of the linear-like region of the concentration-dependent γ_{lv} curve (i.e., the surface excess region between γ^0_{lv} and γ'_{lv} centered at ln $C_B^{\Pi/2}$; see Figure 1) corresponding to steady state, as described previously.[35,36] The term "apparent" alerts the reader to the fact that casual application of Gibbs' adsorption isotherm [$\Gamma = (-1/RT)d\gamma_{lv}/d \ln C_B$] treats solutes (proteins and surfactants) as isomerically pure, nonionized polyelectrolytes[44] at infinite dilution with unit

(42) Schwartz, A. M.; Perry, J. W. *Surface Active Agents*; Interscience: New York, 1949.
(43) Rosen, M. J. *Surfactants and Interfacial Phenomena*; Wiley: New York, 1978.
(44) Frommer, M. A.; Miller, I. R. *J. Phys. Chem.* **1968**, *72*, 2862.

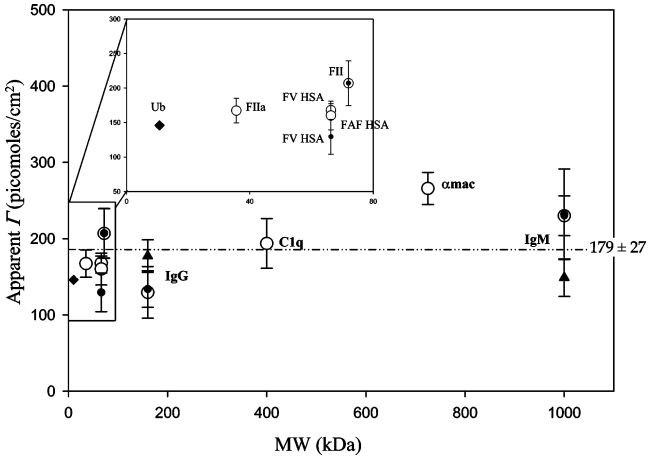

Figure 3. Apparent Gibbs' surface excess Γ as a function of protein MW calculated from concentration-dependent γ_{lv} for multiple preparations of proteins as listed in Table 1 (open circles = preparation 1, filled circles = preparation 2, filled triangles = preparation 3); the inset expands the low-MW region. The data point corresponding to ubiquitin (Ub, filled diamond) was estimated as described in the Appendix, section 6.2. Error bars represent the uncertainty computed by propagation of experimental errors into compiled Γ values (see Results and Discussion). The dashed line represents the arithmetic mean of the Γ values listed in Table 2.

activity coefficients.[39] In particular, this treatment does not explicitly take into account counterions which, for a 1:1 ionic surfactant such as AOT dissolved in pure water, means that the actual surface excess $\Gamma_{lv} = 1/2\ \Gamma$.[43,45] Thus, $\Gamma = 460 \pm 31$ pmol/cm^2 derived from data of Figure 1A was found to be in good agreement with results from drop-volume tensiometry ($\Gamma_{lv} = 221$ pmol/cm^2) and predicts an adsorbed footprint $1/\Gamma_{lv} = 70$ Å^2/molecule in reasonable agreement with neutron reflectometry (NR) measurements.[45,46] No counterion correction of apparent surface excess Γ was necessary for polyelectrolytes dissolved in swamping concentrations of buffer salts,[43] however, and values listed in Table 2 were taken to be proportional to the actual Gibbs' surface excess Γ_{lv}, as discussed in the theory section, bearing in mind, of course, the aforementioned assumptions of purity and applicability of the infinite-dilution approximation.

Figure 3 plots apparent Γ values collected in Table 2 against protein MW, with error bars representing intraexperiment uncertainty calculated by propagation of fitted-parameter errors, as described previously.[35,36] Interexperiment error suggested by replicate protein preparations (sometimes different lots obtained from different vendors, see Table 1) appeared not to be significantly larger than intraexperiment uncertainty. Taken as a whole, these data support the contention that the concentration dependence of interfacial tension $d\gamma_{lv}/d \ln C_B$ was relatively constant among proteins with MW spanning nearly 3 orders of magnitude (10−1000 kDa). Again, in view of the substantial structural diversity of the human plasma proteome sampled by the proteins of Table 1,[31] it seems reasonable to conclude that variability in protein structure does not confer widely varying LV interfacial activity.

4.2. Theoretical Interpretation of Results. Secure interpretation of concentration-dependent interfacial tensions in terms of adsorbed concentrations and interphase thicknesses is critically dependent on the availability of solvent[39] and solute activities[47] for protein solutions of particular interest to this work, as well as packing densities within a 3D interphase. Specific information of this kind is, for the most part, unavailable, and much of the existing protein-adsorption literature is quite controversial or internally inconsistent (see ref 3 and citations therein). Interpretive problems are exacerbated by the fact that only a narrow range of protein MW has been heretofore explored, concentrating work on relatively low-MW proteins[31] such as albumin, lysozyme, and casein and thus comparing proteins derived from different tissues (e.g., blood, ocular, mammary) and sometimes from different species (e.g., bovine vs human). On occasion, chemically treated proteins are used as surrogates for natural forms, such as in the delipidization of fraction (FV) albumin to fatty-acid-free (FAF) serum albumin. This work is exceptional only in that it has specifically focused on purified human globular proteins with a broad range of molecular weights. Even so, a standard of reference is required to (partially) compensate for unknown protein activity. Thus, we have chosen to "calibrate" the model outlined in the theory section to the NR of FAF HSA at the LV interface reported by Lu et al.,[48] recognizing that this single-point calibration to delipidated protein may bias the outcome but with the expectation that any such bias will be systematic and that general trends revealed will not be seriously compromised.

Protein Packing within the LV Interphase. NR resolved a single molecular layer of FAF HSA at the LV interface at saturating surface coverage, residing within a 4.8 nm thick layer.[48] This finding is somewhat consistent with a protein-sphere radius $r_v = 2.7$ nm calculated from molecular-packing density calculations discussed in the theory section or, as described in the cited NR literature, a 4 × 14 nm ellipsoidal molecule adsorbed with the major axis oriented parallel to the interface. The adsorbate mass/unit area deduced from NR was 2.1 ± 0.3 mg/m^2 or 3.2 pmol/cm^2 and was construed to be equivalent to the Gibbs' surface excess Γ_{lv}.[49] Interpreted in terms of eq 9 of the sphere-packing model, this implies that $\Omega^{max} = 4.8 \times 10^{-7}$ cm and that $C_I^{max} = \Gamma_{lv}/\Omega^{max} = 6.7 \times 10^6$ pmol/cm^3 (6.7×10^9 pM or $\ln C_I^{max} = 22.6$ for comparison with the scaling of Figures 1, 2, and 5). With $C_{FCC} = 1.5 \times 10^{10}$ pM for HSA ($\ln C_{FCC} = 23.4$), this implies that $\epsilon \sim 0.45$ or that the saturation interfacial concentration is approximately half of the hypothetical face-centered-cubic arrangement of hard spheres with radius r_v, or $\Phi_p^{max} = 0.74\epsilon \sim 1/3$. The effective-packing radius R is thus 30% larger than r_v with $\chi = 1.3$ (as calculated from $\delta = 2R = 2r_v\chi = 2r_v\epsilon^{-1/3} = 7.1$ nm), which is consistent with a 3.6 nm hydrodynamic radius obtained by dynamic light scattering of albumin solutions.[50] This inferred value of ϵ might also be compared to the so-called "jamming limit" of 0.55 at which adsorbing disks saturate a surface without overlap[51] and to reports of adsorbed-protein densities exceeding this limit,[30,52] so long as it is borne in mind that these latter benchmarks are specific to molecular packing within a single layer (2D) and not in multiple layers (3D). It is of further interest that C_I^{max} exceeds the estimated solubility limit for HSA

(45) Nave, S.; Eastoe, J. *Langmuir* **2000**, *16*, 8733.
(46) Drop-volume measurements are assumed to closely correlate with early pendant-drop measurements taken near $t = 0$ because, in a drop-volume experiment, the LV interface is continuously forming until the drop separates from the tip, rather than achieving the steady-state adsorption condition accessible to an aged pendant drop (Γ = 337.3 ± 28.2 pmol/cm^2 at steady state taken near 1 h drop age).
(47) Rao, C. S.; Damodaran, S. *Langmuir* **2000**, *16*, 9468.
(48) Lu, J. R.; Su, T. J.; Penfold, J. *Langmuir* **1999**, *15*, 6975.
(49) Note that the surface excess of the small-molecule reference compound AOT (MW = 444 Da) reported herein is much larger than that of proteins (1000 < MW < 10 kDa), presumably because of the great disparity in molecular size.
(50) Helfrich, J. P. *Am. Biotechnol. Lab.* **1998**, *16*, 64.
(51) Feder, J. *J. Theor. Biol.* **1980**, *87*, 237.
(52) Robeson, J. L.; Tilton, R. D. *Langmuir* **1996**, *12*, 6104.

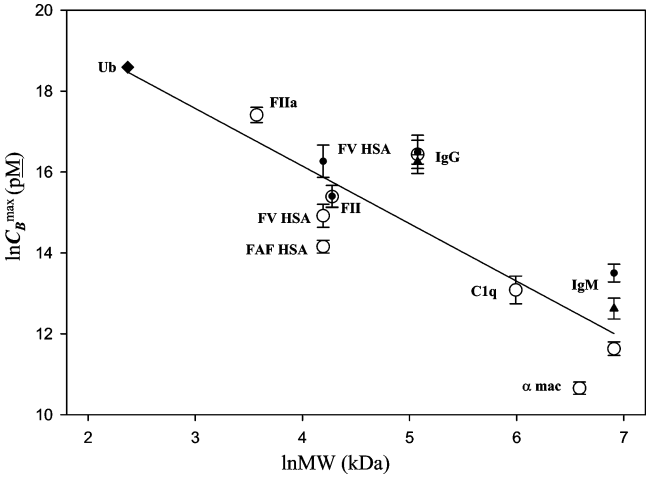

Figure 4. Relationship between the surface-saturating bulk-solution concentration C_B^{max} and protein MW (open circles = preparation 1, filled circles = preparation 2, filled triangles = preparation 3). Linear regression through the data yielded a slope of -1.4 ± 0.2 consistent with the expectation of unit slope and an intercept of 21.8 ± 1.3 ($R^2 = 71.6\%$). Notice that low-MW proteins require greater bulk-phase concentrations to saturate the interphase than higher-MW proteins.

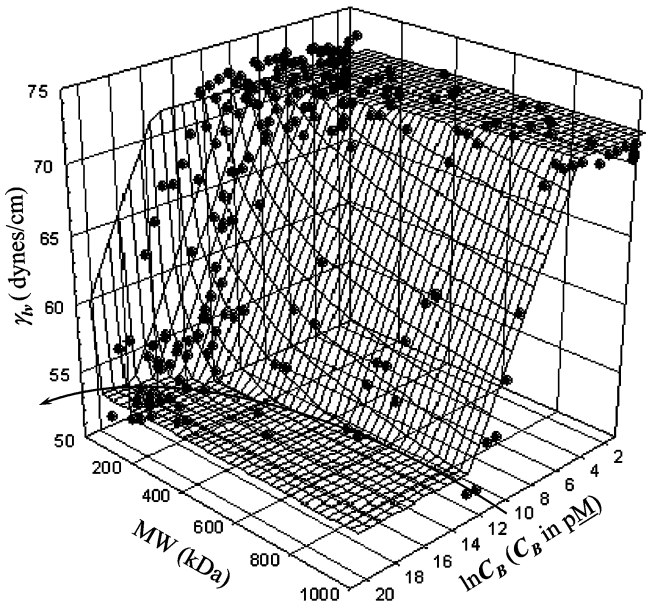

Figure 5. Traube-rule-like dependence of concentration-dependent γ_{lv} for proteins selected from Table 1 spanning 3 decades in MW (reading from left to right on the MW axis: Ub, FIIa, FAF HSA, FV HSA preparation 1, FII preparation 1, IgG preparation 2, α mac, C1q, IgM preparation 4). Data points are superimposed on a mesh calculated from eq 4a of the theory section (see the Appendix, section 6.3, for details). The Traube rule effect is especially evident as viewed along the ln C_B axis where monotonically increasing concentrations of lower-MW proteins are required to reach a universal limiting interfacial tension γ'_{lv}.

by a factor of ~9 ($C_{SL} = 7.5 \times 10^8$ pM, ln $C_{SL} = 20.4$ pM or about 50 g/L), corroborating the conclusion drawn from diverse literature sources that adsorbed concentrations can be surprisingly large and that a proteinaceous interphase must indeed be a very viscous region.[3] We estimate from steady-state concentration-dependent γ_{lv} for FAF HSA that ln $C_B^{max} = 14.2 \pm 0.2$ (1.5×10^6 pM; see Figure 1B and Table 2) suggesting that $P = (C_I^{max}/C_B^{max}) \sim 5 \times 10^3$, which is in reasonable agreement with early ellipsometric measurements of bovine albumin[53] and other related studies reviewed in ref 3. Furthermore, this single-point calculation of P is consistent with the extrapolated value derived from the Traube-like rule for proteins (see below), suggesting that the partition coefficient is approximately constant across the proteins of this study as deduced from the slight variation in $d\gamma_{lv}/d \ln C_B$.

A Traube-like Rule for Protein Adsorption and Partition Constant. Figure 4 plots the C_B^{max} data compiled in Table 2 on logarithmic coordinates compatible with eq 3 of the theory section (the data corresponding to ubiquitin were estimated as described in the Appendix, section 6.2). Proteins fall within a monotonically decreasing band consistent with the anticipation of a unit slope and positive intercept [ln $C_B^{max} = (-1.4 \pm 0.2)$ ln MW + (21.8 ± 1.3); $R^2 = 71.6\%$]. Interpretation of these results must take into account that the highly simplified model of adsorption treats proteins as uniform hard spheres and does not attempt to account for structural complexities of real molecules, variations introduced by delipidization (as in the case of FAF HSA), or unfolding (denaturation) that may occur upon concentration within the interphase. Hence the failure of the data to quantitatively adhere to eq 3 is hardly surprising. Nevertheless, it is of interest to estimate $\epsilon/P \sim 3 \times 10^{-3}$ from the nominal intercept value (bearing in mind the large error) and, by assuming $\epsilon \sim 0.45$ from the preceding section, estimate $P \sim 1.5 \times 10^2$, which is within an order of magnitude of the single-point estimate based on NR discussed above. According to eq 3 and Figure 4, low-MW proteins require greater bulk-phase concentrations to saturate the interphase than higher-MW proteins. Given that the C_B^{max} values plotted in Figure 4 approach 10% w/v, it is reasonable to anticipate that extrapolated C_B^{max} values for yet-lower-MW proteins must equal or exceed protein-solubility limits. As a consequence, surface saturation and the related limiting interfacial tension γ'_{lv} are not expected for low-MW proteins at fixed P. In this regard, it is noteworthy that γ_{lv} curves for low-MW proteins such as ubiquitin (10.7 kDa) fail to achieve a limiting interfacial tension at any concentration below the solubility limit[15] (see Figure 4 and further below).

Figure 5 is a summary graphic showing relationships among steady-state γ_{lv}, MW, and concentration of aqueous-buffer solutions of globular proteins. The data points of Figure 5 correspond to proteins selected from Table 1, whereas the mesh was calculated from eq 4a of the theory section using the fitted value of ϵ/P obtained as discussed above and as further detailed in the Appendix, section 6.3. The Traube-rule effect is especially evident as viewed along the ln C_B axis where increasing concentrations of lower-MW proteins are required to reach the limiting interfacial tension γ'_{lv}. γ'_{lv} is not achieved for low-MW proteins such as ubiquitin, as discussed above.

Surface Excess and Interphase Thickness. Again using NR of HSA as a single-point calibration by taking $\Gamma_{lv} = 3.2$ pmol/cm^2, the factor relating actual and apparent surface excess $c = \Gamma/\Gamma_{lv} = 179/3.2 = 56$. Equation 9 can be used to calculate maximum interphase thickness and, from r_v, the number of layers required to contain different size proteins. As shown in Figure 6, interphase thickness increases linearly with MW. The number of layers occupied by protein has been calculated as increasing in steps, although it seems more likely that transitions are not so discrete, more probably partially filling an additional layer before the previous is well packed. However these layers actually populate, eq 9 predicts that at fixed partition

(53) Feijter, J. A. D.; Benhamins, J.; Veer, F. A. *Biopolymers* **1978**, *17*, 1759.

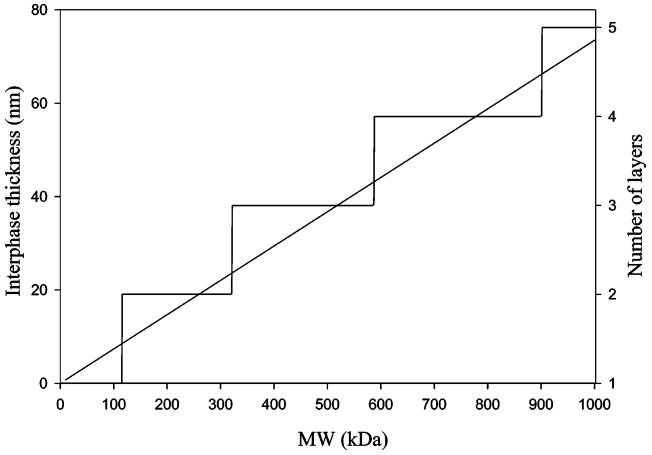

Figure 6. Monotonic increase in interphase thickness with protein molecular weight (left-hand axis). A fixed partition coefficient requires that higher-MW proteins (MW > 125 kDa) occupy multiple layers (right-hand axis), predicting up to five layers for proteins such as IgM (1000 kDa). Transition between layers is shown as occurring in discrete steps although it is more likely that occupation of a subsequent layer occurs before the preceding one is completely packed.

coefficient P, low-MW proteins such as albumin (66 kDa) fall within one layer whereas large proteins such as IgM (1000 kDa) occupy five layers. Thus, the constraint that P is approximately constant for all proteins imposes the requirement that proteins with MW > 125 kDa populate more than a single layer at surface saturation.

5. Conclusions

The two principal experimental observations of this work were that (i) reduction in LV interfacial tension γ_{lv} of aqueous-buffer solutions of purified human proteins followed a regular progression in MW with the molar concentration required to reach a specified value *decreasing* with *increasing* MW and (ii) the rate of change in γ_{lv} with protein concentration $d\gamma_{lv}/d \ln C_B$ was relatively constant among proteins with MW spanning nearly 3 orders of magnitude (10−1000 kDa). The former observation was interpreted in terms of a protein-adsorption model predicated on the packing of spherically shaped molecules with dimensions that scale with MW. The latter was rationalized as an outcome of a constant partition coefficient that entrained a fixed fraction of bulk-solution molecules within a three-dimensional interphase that thickens with increasing protein size (MW). When calibrated to previously reported neutron reflectometry of albumin adsorption to the LV interface, the model permitted calculation of interphase thickness and number of molecular layers residing within this interphase. Interphase thickness was predicted to increase linearly with MW, requiring up to five layers for large proteins (MW ∼ 1000 kDa) but only a single layer for small proteins (MW < 125 kDa).

This study strongly suggests that water orchestrates a systematic pattern in protein adsorption to the LV interface that has not been evident from similar previous studies using proteins covering a narrower MW range. Realization of this pattern has followed a somewhat similar historical pathway to understanding the Traube rule, requiring routine access to purified compounds with known MW spanning a sufficiently large range that homology could be observed. In the protein case, the homology is *molecular size* rather than chemical composition as in the Traube rule, implying that the structural variability that confers vastly different bioactivity to proteins does not greatly affect interaction energetics with water. It is these interactions that lead to the expulsion of protein from solution[14] to the hydrophobic LV interface, simultaneously reducing interfacial energetics and solution concentration of a relatively hydrophobic solute[11] for which water is an ambivalent solvent.[54,55] *Amphilicity* is the word coined by Hartley[56] in 1936 to express this ambivalent solvency from the perspective of the solute molecules (originally amphipathy). Apparently in the case of proteins, molar variability in γ_{lv} is achieved by aggregating greater mass of similar amphiphilic character (blocks of amino acids), as opposed to accumulating greater amphilicity with MW. The extent to which this amphilicity leads to protein accumulation at the LV interface is limited by the extent to which this surface can be dehydrated, interpreted herein as protein volume fraction $\Phi_p^{max} \sim 1/3$. The significance of these conclusions to biomaterials science is that combinations and permutations of the 20 naturally occurring amino acids comprising the primary sequence of mammalian proteins seem insufficient to support widely varying LV interfacial activity, no matter how these sequences happen to fold into higher-order structure. As a consequence, assertion of differential protein adsorption to biomaterial surfaces from heterogeneous biological mixtures (such as blood) based on molecular structure alone requires careful justification in terms of interfacial energetics,[15] bearing in mind that hydrophobic hydration is a, perhaps the, key phenomenon controlling adsorption.

Glossary of Symbols

a	protein activity
A	area of interphase (cm^2)
c	proportionality constant, $c \equiv \Gamma/\Gamma_{lv}$
C_B	bulk-solution concentration (moles/volume)
C_B^{max}	bulk-solution concentration at limiting interfacial tension (moles/volume)
$C_B^{\Pi/2}$	bulk-solution concentration at half-maximal change in interfacial activity (moles/volume)
C_B^*	bulk-solution concentration at arbitrary interfacial tension γ_{lv}^* (moles/volume)
C_{FCC}	face-centered-cubic close-packing concentration (moles/volume)
C_I	interphase concentration (moles/volume)
C_I^{max}	maximal interphase concentration (moles/volume)
C_{SL}	solubility limit concentration (moles/volume)
χ	proportionality constant, $\chi \equiv R/r_v$
δ	interphase thickness element (cm)
ϵ	packing efficiency
Φ_p	volume fraction of protein in the interphase
Φ_p^{max}	maximum volume fraction of protein in the interphase
γ_{lv}	liquid−vapor interfacial tension (dyn/cm)
γ_{lv}^0	low-concentration asymptote of a concentration-dependent γ_{lv} curve (dyn/cm)
γ_{lv}'	high-concentration asymptote of a concentration-dependent γ_{lv} curve (dyn/cm)
γ_{lv}^*	arbitrary interfacial tension (dyn/cm)
Γ_{lv}	actual Gibbs' surface excess (moles/area)
Γ	apparent Gibbs' surface excess (moles/area), $\Gamma = c\Gamma_{lv}$
M	parameter fitted to concentration-dependent γ_{lv} curve

(54) Pain, R. H. Molecular Hydration and Biological Function. In *Biophysics of Water*; Franks, F., Mathias, S., Eds.; John Wiley and Sons: Chichester, 1982; p 3.
(55) Rand, R. P. *Science* **1992**, *256*, 618.
(56) Hartley, G. S. *Actual. Sci. Ind.* **1936**, *387*, 4.

n_I	total protein moles within the interphase (moles), $n_I = n_a + n_B$
n_a	moles of adsorbate within the interphase (moles)
n_B	moles of protein contributed by the bulk phase (moles)
n_1	moles of component 1 in a two-component solution
n_2	moles of component 2 in a two-component solution
N	number of slabs of interphase
N_A	Avogadro number
P	partition coefficient, $P \equiv C_I/C_B$
Π	spreading pressure (dyn/cm), $\Pi \equiv \gamma_{lv}^0 - \gamma_{lv}'$
Π^{max}	maximum spreading pressure (dyn/cm)
r_v	protein radius (cm)
R	effective radius (cm), $R \equiv \chi r_v$
R	universal gas constant (erg/K mol)
σ	activity coefficient
T	temperature (K)
V_I	interphase volume (cm^3)
V_p	protein molar volume (cm^3/mol)
Ω	total interphase thickness (cm)
x	mole fraction

Acknowledgment. This work was supported, in part, by the National Institutes of Health PHS 1 R01 HL 69965-01 and by Johnson & Johnson through the Focused Giving Grant Program. The authors appreciate additional support from the Materials Research Institute and Departments of Bioengineering and Materials Science and Engineering, Penn State University. The authors gratefully acknowledge the assistance of Dr. Roger Woodward in instrument design and implementation.

6. Appendix

6.1. Estimation of C_B^{max}. C_B^{max} was calculated from fitted data by evaluating eq 4a of the theory section at half-maximal change in interfacial tension $\gamma^{\Pi/2} = {}^1/_2(\gamma_{lv}^0 - \gamma_{lv}')$, which occurs at a bulk-phase composition ln $C_B^{\Pi/2}$:

$$\Delta\gamma_{lv}/\Delta \ln C_B = -RT\Gamma = \frac{(\gamma_{lv}' - \gamma_{lv}^*)}{[\ln C_B^{max} - \ln C_B^*]} = \frac{(\gamma_{lv}' - \gamma^{\pi/2})}{[\ln C_B^{max} - \ln C_B^{\pi/2}]} = \frac{\left(\gamma_{lv}' - \left(\gamma_{lv}' + \frac{\Pi^{max}}{2}\right)\right)}{[\ln C_B^{max} - \ln C_B^{\pi/2}]} \Rightarrow$$

$$\ln C_B^{max} = \frac{\Pi^{max}}{2RT\Gamma} + \ln C_B^{\pi/2} \quad \text{(A1)}$$

where the identity $\Pi^{max} \equiv \gamma_{lv}^0 - \gamma_{lv}'$ has been used. All of the parameters on the right-hand side of eq A1 are derived from nonlinear, least-squares fitting of concentration-dependent γ_{lv} to a four-parameter logistic equation as described in Methods and Materials. Confidence in the C_B^{max} values listed in Table 2 and plotted in Figure 4 was computed by propagation of the standard errors in best-fit parameters through eq A1 as given by eq A2. In consideration of all sources of experimental error, we conclude that ln C_B^{max} estimates are no better than about 20%.

$$\sigma^2_{C_B^{max}} = \sigma_{C_B^{\pi/2}}{}^2 + \frac{1}{4(RT\Gamma)^2}\left[\sigma^2_{\gamma_{lv}^0} - \sigma^2_{\gamma_{lv}'} - \left(\frac{\gamma_{lv}^0 - \gamma_{lv}'}{\Gamma^2}\right)^2 \sigma_\Gamma{}^2\right] \quad \text{(A2)}$$

where the σ's represent standard errors in ln C_B^{max} and the best-fit parameters ln $C_B^{\Pi/2}$, γ_{lv}^0, γ_{lv}', and Γ.

6.2. Estimation of Parameters for Ubiquitin. The parameters for ubiquitin (Ub) listed in Table 1 and shown in Figures 2−5 are graphical estimates from the steady-state, concentration-dependent γ_{lv} curve. Firm values could not be ascertained by statistical-fitting procedures described in Methods and Materials because surface saturation is not reached within solubility limits for this protein. Thus, a well-defined high-concentration asymptote γ_{lv}' is not achieved at physically realizable concentrations. However, the highest-concentration $\gamma_{lv} \sim 46$ dyn/cm is within the Π^{max} of all other proteins studied. Given that Π^{max} is conserved among the broad range of proteins, it seems reasonable to conclude that $\gamma_{lv} = 46$ dyn/cm is not too far from the hypothetical γ_{lv}' that would be achieved if Ub was sufficiently soluble to fill the interphase. Thus, we estimate that $\Pi^{max}/2 \sim 13$ dyn/cm would occur at ln $C_B^{\Pi/2} = 15$ pM. The low-concentration asymptote is clearly defined at $\gamma_{lv}^0 = 72$ dyn/cm, consistent with the interfacial tension of saline near 25 °C. An estimate of the apparent surface excess Γ was made from the experimental data by application of the Gibbs' adsorption isotherm. With these estimates in hand, C_B^{max} was calculated as described in section 6.1.

6.3. Steady-State γ_{lv} as a Function of MW and Concentration. The smooth mesh through the summary graphic Figure 5 was computed from eq 4a of the theory section assuming that the nominal values $\gamma_{lv}^0 = 72$, $\gamma_{lv}' = 45$, and $\Gamma = 179$ approximate all proteins of this study. Equation 4a permits calculation on any interfacial tension within the linear-like Gibbs' excess region (i.e., the surface excess region between γ_{lv}^0 and γ_{lv}' centered at ln $C_B^{\Pi/2}$; see Figures 1A and 3), above and below which calculated γ_{lv}'s are truncated to γ_{lv}^0 and γ_{lv}', respectively.

LA035308T